ACS APPLIED ENERGY MATERIALS

www.acsaem.org Article

Influence of Binder Crystallinity on the Performance of Si Electrodes with Poly(vinyl alcohol) Binders

Prithwiraj Mandal, Killian Stokes, Guiomar Hernández, Daniel Brandell, and Jonas Mindemark*

Cite This: *ACS Appl. Energy Mater.* 2021, 4, 3008−3016 Read Online

ACCESS | Metrics & More | Article Recommendations | Supporting Information

ABSTRACT: Silicon is a highly promising electrode material for Li-ion batteries because of its high theoretical capacity, but severe volume changes during cycling leads to pulverization and rapid capacity fading. The use of alternative and water-soluble polymer binders such as poly(vinyl alcohol) (PVA) or poly(acrylic acid) (PAA) can improve the cycling performance of Si-based Li-ion batteries. Here, we investigate the effect of the substitution of the hydroxyl groups of PVA chains by carboxylic acid and acetate groups on the electrochemical performance of Si anodes in Li-ion batteries. Using modified PVAs, a model system is created spanning the chemical space between PVA and PAA, and the role of different Si-adhering functionalities is investigated. When comparing the electrochemical performance of Li-ion battery cells using Si anodes and the investigated binder systems, PVA with the highest degree of hydrolysis exhibits a superior performance (100 cycles with 1019 mAh g^{-1}) compared to modified PVAs and PAA as a binder for Si anodes. An increased degree of hydrolysis of PVA is also seen to be beneficial for high capacity retention. These effects can be largely explained by the crystallinity of the binder system, which renders an improved electrode integrity during cycling and less swelling of the Si particles.

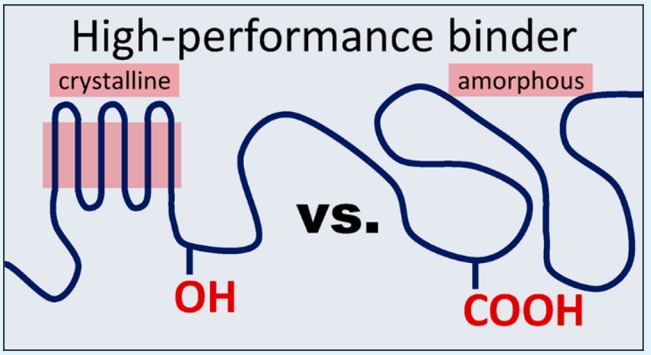

KEYWORDS: *silicon, electrode, binder, Li-ion battery, crystallinity*

INTRODUCTION

Rechargeable lithium-ion batteries (LIBs) are today widely used as electrochemical energy storage devices in consumer electronics, smart grids, and electric vehicles because of their high energy density and long cycle life.[1,2] The components of the electrodes play a significant role in the electrochemical performance of a battery. Traditionally, transition metal oxides (e.g., lithium cobalt oxide)[3] and carbonaceous materials[4] are used as active materials in the positive and negative electrodes, respectively. Due to the low specific capacity of the conventional graphite electrode (ca. 370 mAh g^{-1}), significant efforts have been made in recent years to utilize alternative electrode materials. Alloy anodes such as Al, Si, Ge, Sn, and Sb are in this context highly promising because of their high specific and volumetric energy densities.[5] Compared to the other alloy anode materials, Si makes a natural choice due to its high theoretical capacity (4200 mAh g^{-1}), low operating potential, natural abundance, and environmental benignity. However, severe problems in terms of capacity fading, poor rate capability, and short cycle life limit the commercial adoption of Si-based electrodes.[6−8] Some of these are connected to the severe volume changes (expansion and contraction) that the silicon particles experience during cycling which lead to pulverization of the active material particles, continuous growth of the SEI layer thickness, and loss of electrical contact with the current collector and ultimately to a fast capacity drop after a limited number of cycles.

To improve the electrochemical performance of Si anodes, various strategies using nanostructured silicon materials have been explored, such as Si nanowires,[9,10] nanotubes,[11] core−shell structures,[12,13] and porous nanomaterials.[14−16] Although these materials have been shown to significantly improve the cycling performance of the Si anode, their preparation is complicated and often involves a multistep process to obtain the particular structures, which is less suitable for large-scale industrial applications. Alternative approaches to improve the stability of Si-based anodes include the use of functional polymer binders. The polymer binder, an inactive but major component in any LIB electrode, plays an important role for maintaining the structural, mechanical, and electrical integrity of the electrode while it also plays a key role in developing the formation of a stable SEI layer.[17−22] Not only does the chemical identity of the binder have a profound influence on

Received: August 24, 2020
Accepted: March 23, 2021
Published: April 2, 2021

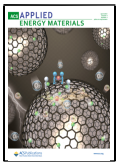

the performance of the electrodes, but also the properties such as the molecular weight and the rheological properties during processing are important parameters to consider.[23,24] While poly(vinylidene fluoride) (PVdF) has traditionally been used for conventional graphite electrodes,[25] for Si, hydrogen-bonding polymers that are soluble in water and can interact with the silanol groups on the surface of the Si particles are preferred.[26] This could be polymers bearing either carboxyl (−COOH) groups, such as in poly(acrylic acid) (PAA),[23,27,28] or hydroxyl (−OH) groups, such as in carboxymethyl cellulose (CMC)[29,30] or poly(vinyl alcohol) (PVA).[31]

On their own, both −COOH and −OH moieties are useful for high-performance binders for Si anodes; e.g., both PAA and PVA have been demonstrated to be good binders for Si anodes. Because of the high concentration of H-bonding −COOH groups, PAA exhibits better cycling performance compared to PVdF and CMC.[32] Meng et al. reported 80% capacity retention of Si anodes containing PAA after 100 cycles as compared to 73% for CMC.[28] When it comes to the comparison between PAA and PVA, the reported results are somewhat contradictory,[18,33,34] possibly because of different amounts of binder and different mass loadings in the electrodes. Moreover, since PVA is prepared by hydrolysis of poly(vinyl acetate) and thereby contains a variable amount of residual acetate groups, the degree of hydrolysis may also have an effect on the cycling performance of anodes prepared with PVA as the binder. This raises the question of the relative roles of these different functionalities in the binder for the battery performance and how these can be utilized to design and tailor binders with optimized properties for the efficient cycling of Si anodes. Recently, the development of multifunctional polymer binders,[33] such as alginate[35] or dopamine-grafted PAA,[36] having both −OH and −COOH groups in the polymers with further improved performance of the Si anodes has been reported. Wang et al. further reported an interpenetrated gel polymer binder prepared by PVA and PAA for high-performance Si anodes.[37]

For a closer investigation of the influence of hydrogen-bonding functionalities in the binder on cycling performance, the chemical space spanned by PVA and PAA is a relevant model system, since it essentially describes a continuum between a purely hydroxyl-functional to a purely carboxyl-functional material. By investigating the intermediate structures, comprising both functionalities, as well as PVAs with different degrees of functionality, we have here explored the function of PVA as a binder and the relative influence of hydroxyl and carboxyl functionalities in the binder on the performance of Si anodes. In contrast to much of the other work published on similar systems in literature, we also investigate the electrochemical performance of Si anodes using a low binder content, to better put these electrodes in the context of industrial applications. Paradoxically, we show that the cycling performance of the electrodes is not strictly related to the functionality of the binder but rather to its resulting morphology, where pristine PVA with a high degree of hydrolysis—and high crystallinity—outperforms the rest of the binders in terms of cycling efficiency and capacity retention.

EXPERIMENTAL SECTION

Materials. Poly(vinyl alcohol) (13−23k, degree of hydrolysis 98% or 87−89%, Aldrich; 9−10k, degree of hydrolysis 80%, Aldrich), poly(acrylic acid) (35 wt % solution in water, Aldrich, Mw = 250 000 g/mol), 4-dimethylaminopyridine (DMAP), maleic anhydride, and succinic anhydride were purchased from Aldrich.

Preparation of Carboxyl-Modified of PVA Polymer Binder. In a 50 mL round-bottom flask, 1.0 g of PVA-98 (degree of hydrolysis 98%) (0.0227 mol, based on the $-CH_2-CH(OH)-$ repeating unit) and 10 mL of deionized water were added. The solution was heated at 95 °C for 15 min to dissolve the PVA, and of temperature was then decreased to 65 °C. Dimethylaminopyridine (DMAP) (0.2776 g, 0.00227 mol) was added to this solution and stirred for 1 h. Maleic anhydride (3.343 g, 0.0341 mol, 1.5 equiv) was added, and the mixture was stirred at this temperature for 24 h. The solution was cooled to room temperature, another 10 mL of deionized water was added, and the product was precipitated in acetone followed by washing twice with acetone. Finally, the polymer was dried in vacuum for 3 days (degree of modification = 6% according to NMR). Another three reactions were carried out (using 0.5, 1.0, and 2.0 equiv of maleic anhydride with respect to the molar ratios of PVA) under similar reaction conditions, resulting in degrees of modification of 2%, 5%, and 11% respectively. Typical yields were about 0.96 g. ^{1}H NMR (DMSO-d_6): δ (ppm) = 6.2−6.4 (2H, $-CH{=}CH-$), 5.1 (1H, $-CHOCO-$), 3.7−3.9 (1H, -CHOH), 1.2−1.6 ($-CH_2-$).

The chemical modification of PVA using succinic anhydride (1.0 and 1.5 equiv with respect to the molar ratios of PVA) was carried out in similar way and under the same reaction conditions, resulting in degrees of modification of around 2% and 2.2%, respectively.

Electrode Preparation. Silicon electrodes were prepared by mixing nanosilicon powder (≤50 nm, Alfa Aesar), Super P C-65 carbon black, and polymer binder in a weight ratio of 80:10:10 or 82:13:5 in deionized water. The mixture was stirred for 1 h in a ball mill to form a homogeneous slurry. The electrode slurry was coated onto the surface of a Cu foil with a stainless-steel notch bar and was allowed to dry for 24 h under atmospheric conditions. The electrodes were finally transferred to an Ar-filled glovebox and dried in a vacuum oven at 80 °C for 12 h. The electrode film was cut into 13 mm disks used for the electrochemical tests. The mass loading of Si nanoparticles of all electrodes after drying was in a range of ∼0.7−0.85 mg cm^{-2}.

Electrochemical Characterization. The electrochemical properties of the prepared samples were measured using CR2025 coin-type cells. Solupor was used as the separator and lithium foil was used as the counter electrode. The coin cells were assembled in a high-purity argon-filled glovebox, and the electrolyte was made of 1.0 M lithiumhexafluorophosphate ($LiPF_6$) in a mixture of ethylene carbonate/ethylmethyl carbonate (volume ratio of EC/EMC = 3:7) (Gotion) with 10 wt % fluoroethylene carbonate (Gotion) and 2 wt % vinylene carbonate (Gotion). The electrochemical tests were performed on an Arbin Test System in galvanostatic mode at room temperature. The voltage range was 0.01−1.5 V for all tests. The first cycle was performed at a C-rate of C/20, and then the C-rate was changed to C/10 for the subsequent cycles. The measured capacities were determined based on the mass of the active Si material on the electrode. In the case of the electrodes with 5 wt % pristine PVA binders of different degrees of hydrolysis, the first cycle was run at C/20 and the subsequent cycles were run at C/5.

Materials Characterization. ^{1}H NMR spectra were recorded on a JEOL ECZ 400S 400 MHz spectrometer at room temperature using DMSO-d_6 or D_2O as the solvent. FTIR analysis was carried out using a PerkinElmer Spectrum One FT-IR spectrometer with an attenuated total reflectance (ATR) accessory. Thermal degradation of the polymer samples was studied using thermogravimetric analysis (TGA) on a TA Instruments TGA Q500. Samples were heated from 25 to 600 °C at a heating rate of 10 °C/min under a nitrogen atmosphere. Differential scanning calorimetry (DSC) analysis was performed on a TA Instruments Q2000 using a heat−cool−heat procedure between 25 and 250 °C at a rate of 10 °C/min under a nitrogen atmosphere. The temperature against the heat flow was recorded. The morphology of the uncycled Si electrodes was obtained by scanning electron microscopy (Zeiss-1550) with an accelerating voltage of 3 kV. For the cycled electrodes, cells were disassembled in an Ar-filled glovebox before being washed with a small quantity of

https://doi.org/10.1021/acsaem.0c02051
ACS Appl. Energy Mater. 2021, 4, 3008−3016

Scheme 1. Chemical Modification of PVA-98 by Carboxylic Acid Anhydrides

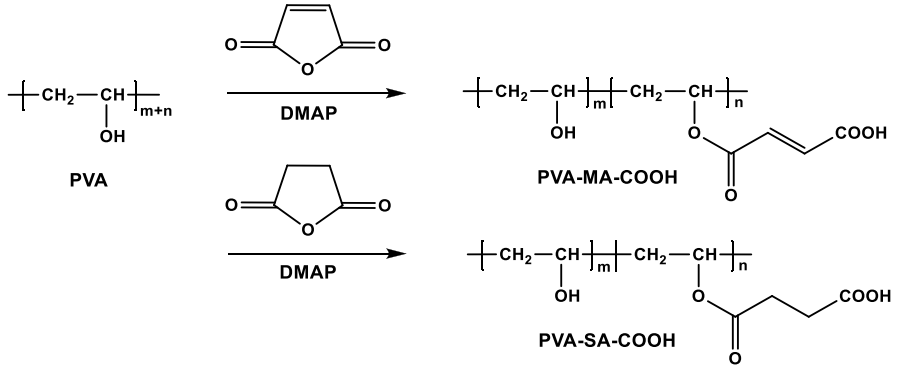

dimethyl carbonate (DMC) to remove excess electrolyte. The samples were then placed in an inert vacuum-sealed transfer chamber to ensure that the samples were not exposed to air before being transported to the SEM. The cycled material was imaged at an accelerating voltage of 3 kV in a Merlin field-emission SEM (Zeiss). Rheological characterization was performed using a TA Instruments AR2000 using a 2°, 40 mm diameter stainless-steel cone geometry. The measurements were conducted at 25 °C in air with a solvent trap used to maintain an atmosphere of saturated humidity and minimal sample evaporation. All samples were first subjected to a frequency sweep with a controlled strain of 1% in the frequency interval 0.1−10 Hz. Subsequently a steady-state flow experiment was performed at a series of controlled shear rates.

RESULTS AND DISCUSSION

Both PVA and PAA have previously been successfully applied as binders in Si anodes for Li-ion batteries. In this context, PVA is a water-soluble semicrystalline polymer having numerous hydroxyl groups. The hydroxyl groups of PVA can participate in H-bonding with both the active materials and the current collector, and its high adhesion has been shown to lead to high capacity retention during cycling of Si/graphite composite anodes.[31] On the other hand, PAA is amorphous and stiff and has a large amount of −COOH groups in the chains which are believed to be the reason for the high cycling performance observed when PAA is used as the binder in Si anodes.[18,27,32] Since both hydroxyl and carboxyl groups can apparently contribute to improving the cycling performance of Si-containing anodes, the relative effect of these functional groups becomes a relevant question, as well as what would be the optimal binder composition in terms of these functionalities.

The presence of the reactive −OH groups in PVA provides a suitable point of modification that may be used to tune the properties of this polymer. By the substitution of −OH groups with −COOH groups in PVA, the chemical space between PVA and PAA in terms of functional groups may be explored. To this end, we carried out the substitution of −OH groups with −COOH groups in PVA by the reaction with two cyclic carboxylic acid anhydrides—maleic anhydride and succinic anhydride—according to Scheme 1. Since commercial PVA is produced by the hydrolysis of poly(vinyl acetate), different grades of PVA differ in terms of their degree of hydrolysis (i.e., the amount of residual acetate groups in the structure). To avoid the effects of residual acetate groups, a PVA with a high degree of hydrolysis (98%) was used, henceforth referred to as PVA-98.

The chemical modification of PVA-98 was carried out in deionized water using dimethylaminopyridine (DMAP) as catalyst and maleic anhydride (MA) and succinic anhydride (SA) as carboxylating agents (Scheme 1), and the subsequently carboxylated PVAs are referred to as PVA-COOH-MA-0.5, PVA-COOH-MA-1.0, PVA-COOH-MA-1.5, PVA-COOH-MA-2.0, PVA-COOH-SA-1.0, and PVA-COOH-SA-1.5 with the numbers referring to the number of equivalents of the carboxylating agent used in the synthesis. The structures of the modified PVAs were confirmed by ^{1}H NMR and FTIR spectroscopy. Figure 1 shows the ^{1}H NMR spectroscopy of

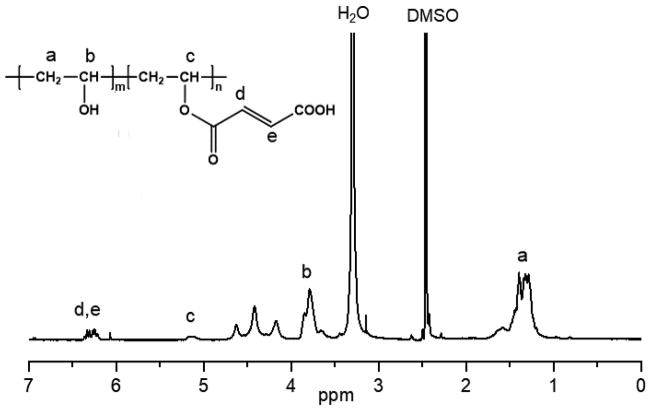

Figure 1. ^{1}H NMR spectrum of carboxylated PVA (PVA-COOH-MA-1.5).

PVA-COOH-MA-1.5. The resonances at 6.2−6.4 ppm are due to the unsaturated protons, designated as "d" and "e", respectively. The resonances at 5.1 ppm are due to the −C**H**OCO− protons designated as "c". The resonances at 3.7−3.9 and 1.2−1.6 ppm are due to the −C**H**OH and −C**H**$_2$− protons, respectively (designated as "b" and "a", respectively). The resonances at 6.2−6.4 and 5.1 ppm thereby indicate the successful modification of PVA by maleic anhydride. The extent of carboxylation was calculated by comparing the integral areas between "c" and "b", which was determined to be 6% for this particular polymer and ranged from 2−11% for the other MA-modified PVAs (Table 1). Compared to the MA-modified PVAs, the degrees of modification of the SA-modified PVAs were lower (around 2%), likely due to a lower solubility of succinic anhydride in water.

FTIR spectra of the PVA and the carboxylated PVA polymers modified by MA and SA are shown in Figure 2. The modified PVA exhibits new peaks at 1713 and 1175 cm^{-1}, which are attributed to the stretching of the carbonyl group

https://doi.org/10.1021/acsaem.0c02051
ACS Appl. Energy Mater. 2021, 4, 3008−3016

Table 1. Degree of Modification of PVA-98 Using Different Carboxylic Anhydrides

sample	degree of modification of PVA-98 (%) (determined from ^{1}H NMR)
PVA-COOH-MA-0.5	2.0
PVA-COOH-MA-1.0	5.0
PVA-COOH-SA-1.0	2.0
PVA-COOH-MA-1.5	6.0
PVA-COOH-SA-1.5	2.2
PVA-COOH-MA-2.0	11.0

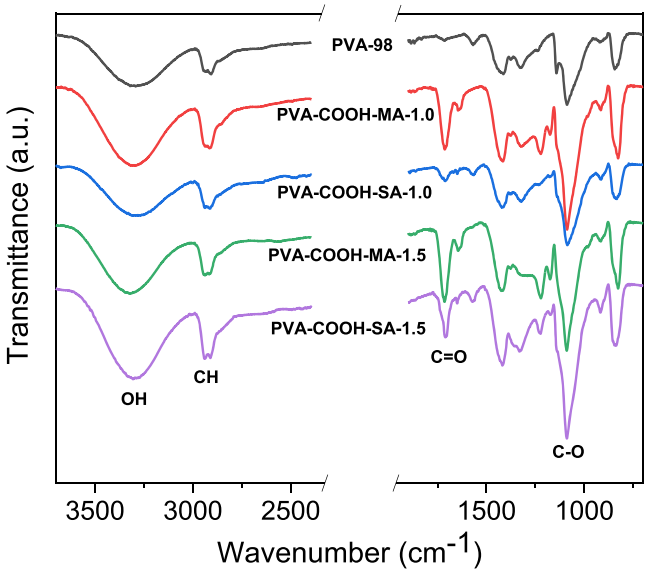

Figure 2. FTIR spectra of unmodified and modified PVAs.

and C−O stretching of the ester moiety, respectively. These new peaks further confirm the successful carboxyl modification of PVA.

To obtain better insights into the interaction between the active electrode material and the modified PVA, FTIR spectra were also recorded of a slurry of PVA-COOH together with Si particles. To this end, commercial nanosilicon powder with an average size of ∼50 nm was used. The Si nanoparticles were covered with a native thin layer of amorphous SiO_2 which was confirmed by FTIR spectroscopy as shown in Figure S1.[26,37] It can be seen that the FTIR spectrum of the pristine Si nanoparticles displays peaks at 1139 and 877 cm^{-1}, which can be attributed to the asymmetric stretching band of Si−O−Si and the symmetric stretching band of Si−O, respectively. Moreover, the broad peak at 3000−3600 cm^{-1} indicates hydrogen bonding of the Si−OH groups. Figure 3a shows the FTIR spectra of a mixture of PVA-COOH-MA-1.0 and Si active particles, coated on Cu foil from a slurry prepared in deionized water. A shift of the C═O stretching frequency of the side groups from 1713 cm^{-1} to the lower wavenumber of 1699 cm^{-1} can be observed, whereas the characteristic band at 2927 cm^{-1}, which is typical for C−H stretching, experienced no shift. This indicates that there are interactions of −COOH groups of the modified PVA with the active material particles, as illustrated in Figure 3b. The shift toward lower wavenumbers is the opposite of what would be expected from the formation of esters or carboxylic anhydrides; this implies that the interactions are primarily noncovalent. These interactions between the binder and the active material particles are

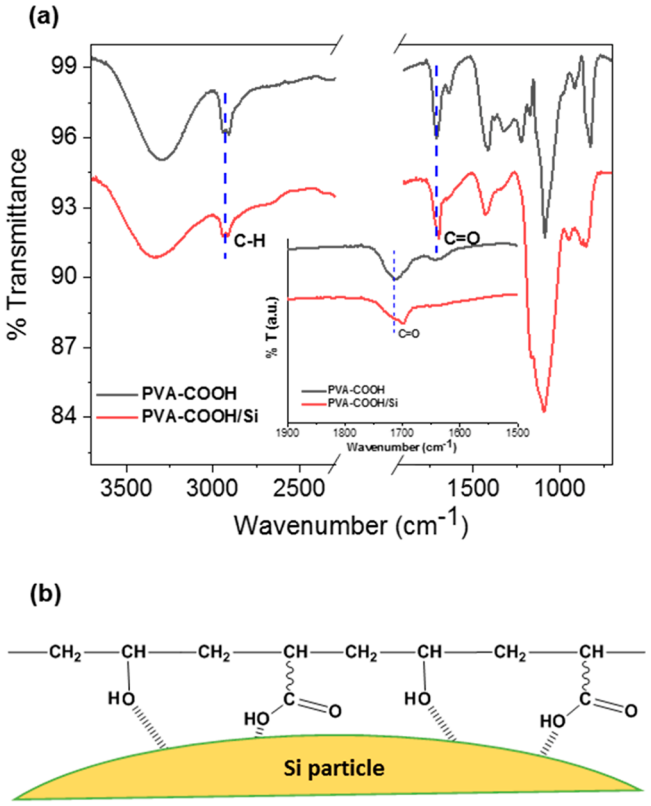

Figure 3. (a) FTIR spectra of PVA-COOH-MA-1.0 and a mixture of PVA-COOH and Si coated on Cu foil and (b) possible interactions between PVA-COOH and Si particles.

expected to be beneficial for the improvement of the stability of the electrode during cycling, as they help to preserve the integrity of the electrodes during volume expansion of the Si particles and ensure keeping the electrical contact between the active particles and the current collector intact.

Having established the structure of the modified PVAs and their interactions with the Si nanoparticles, the effects of the different binders on the electrochemical performance of the Si anodes were evaluated by fabricating coin cells with a lithium foil as the counter electrode. Galvanostatic charge−discharge tests of the silicon electrodes were conducted in the voltage range of 0.01−1.5 V with the results shown in Figure 4.

While there is an initial marked decrease in capacity for all cells, this is expected due to SEI formation and amorphization of the Si during early cycling.[38,39] The first ∼20 cycles may thus be considered as an extended stabilization period in this context. A more interesting comparison between the different materials is instead to look at the long-term capacity retention. What is striking is the remarkable performance by the pristine PVA-98 binder, which displays a capacity retention that is superior to any of the other binders, amounting to a long-term capacity of 1019 mAh g^{-1} after 100 cycles at C/10 (1C = 3579 mAh g^{-1}). In contrast, both the modified PVAs and PAA binders give notably lower capacities after 100 cycles (509 mAh g^{-1}, 637 mAh g^{-1}, 451 mAh g^{-1}, 616 mAh g^{-1}, and 473 mAh g^{-1} for PVA-COOH-MA-1.0, PVA-COOH-SA-1.0, PVA-COOH-MA-1.5, PVA-COOH-SA-1.5, and PAA, respectively). Individual plots of the average charge capacities of the three cells with standard deviations are shown in Figure S2, and the corresponding capacity values can be found in Table S1. The coulombic efficiency (Figure 4b) is also higher

https://doi.org/10.1021/acsaem.0c02051
ACS Appl. Energy Mater. 2021, 4, 3008−3016

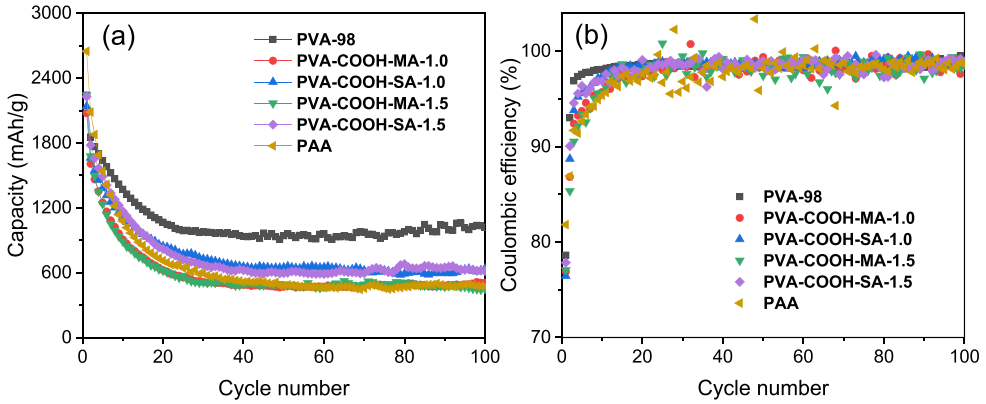

Figure 4. (a) Specific capacity (average of three cells) as a function of cycle number for the Si anode comprising 10 wt % PVA, PVA-COOHs, and PAA binders at C/20 (1st cycle) and C/10 (subsequent cycles); (b) coulombic efficiency plotted as a function of cycle number.

for the unmodified PVA-98, reaching 93.0% in the first cycle at C/10 and 98.2% after 10 cycles, compared to 85.3−90.0% in the first cycle at C/10 and 95.7−97.6% after 10 cycles for the modified materials and PAA.

The results clearly show the potential of PVA in itself as a high-performance binder, capable of supporting a very stable cycling with an average capacity of 1019 mAh g^{-1} after 100 cycles. This is notably superior to PAA, which performs relatively poorly under these conditions. Contrary to for PAA, reports regarding the use of PVA as a binder for Si anodes are comparatively scarce.[23,27,28] Park et al. reported better cycling performance with high-MW PVA for Si/C anodes due to strong H-bonding compared to PAA as a binder.[31] Another study also reports the better performance of PVA compared to PAA as binders for the Si anodes and reported 38.5% and 31.9% capacity retention for PVA and PAA respectively at a current density of 400 mA g^{-1} for 150 cycles.[34] Jeena et al. also reported better cycling performances of PVA compared to PAA in Si anodes comprised of 20 wt % binders with capacities of around 1250 mAh g^{-1} and 700 mAh g^{-1}, respectively, after 70 cycles.[33] These earlier results largely support the finding in this current and more systematic study.

The trend among the modified materials seems to superficially follow the degree of modification such that a higher amount of carboxyl functionalities is equivalent to a lower capacity retention. As an example, the SA-modified PVAs, with a comparatively low degree of modification, consistently perform better than the MA-modified PVAs. However, the difference in long-term capacity retention between the two MA-modified PVAs and PAA is largely negligible despite the clear difference in the chemical functionalities of these materials. If PVA-COOH-MA-0.5 and PVA-COOH-MA-2.0 (Figure S2) are additionally included in the discussion, this discrepancy becomes even more obvious. It should also be noted that the degrees of modification of the PVAs is rather low—not exceeding 11%. Still, the cycling performance drops sharply even at these low degrees of functionalization. Indeed, while there is a clear correlation between performance and the degree of functionalization of the PVA binders in that the modified materials show poorer performance, there is no distinct correlation between performance and the type of functionality. This is surprising, considering that these functionalities are responsible for the interactions between the binder and the active material particles, as indicated by the FTIR data discussed earlier. Understandably, −OH and −COOH groups do not interact with the Si particles in an identical fashion. As a consequence, the adhesion strength of the electrode coatings may differ between the different materials and have an influence on the observed performance. However, the significant drop in performance even at low degrees of modification suggest that the explanation for the cycling performance observed with these materials needs to be sought elsewhere.

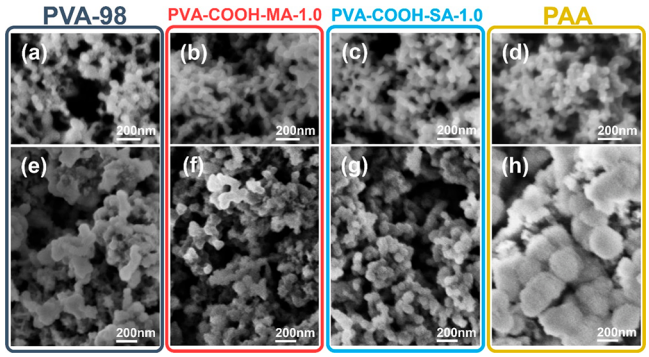

Figure 5. SEM images of Si electrodes at high magnification using (a, e) PVA-98, (b, f) PVA-COOH-MA-1.0, (c, g) PVA-COOH-SA-1.0, and (d, h) PAA as binders (a−d) before and (e−h) after cycling at C/20 (1st cycle) and C/10 (subsequent cycles) for a total of 100 cycles. The corresponding cycling data can be found in Figure S3.

The structural effects of long-term cycling on the Si electrodes can be seen in the SEM micrographs in Figure 5. After 100 charge−discharge cycles, the PAA electrode (Figure 5h) stands out, showing a more pronounced increase in size of the particles. Since no visible cracks can be seen, a large part of this volume can be surmised to consist of electrolyte degradation products. This suggests a poorer ability of the PAA binder to protect the particle surface against electrolyte degradation, leading to excessive SEI formation. In contrast, no major differences can be noted among the PVA binders (Figure 5e−g).

If the explanation of the cycling behavior cannot be found in the *chemical* structure of the binders, perhaps the answer instead lies in the *morphological* structure? Since the most defining morphological feature of PVA is its high crystallinity,[40] the thermal properties of the binders were determined. The melting temperature of PVA is known to be close to the degradation temperature of the material.[41,42] Additionally, the modified materials may undergo ring formation by the

https://doi.org/10.1021/acsaem.0c02051
ACS Appl. Energy Mater. 2021, 4, 3008−3016

carboxylic acid side groups at elevated temperatures to re-form the cyclic anhydride reagent. Naturally, this may complicate the determination of the crystallinity and melting points of the PVA and modified PVA materials. As seen in the TGA thermograms in Figure S4, there is a gradual weight loss, probably due to adsorbed atmospheric water, with the onset temperature of major degradation generally exceeding 200 °C. Indeed, this is very close to the melting endotherm of PVA-98 at 211 °C, as determined by DSC (Figure 6). As can be seen,

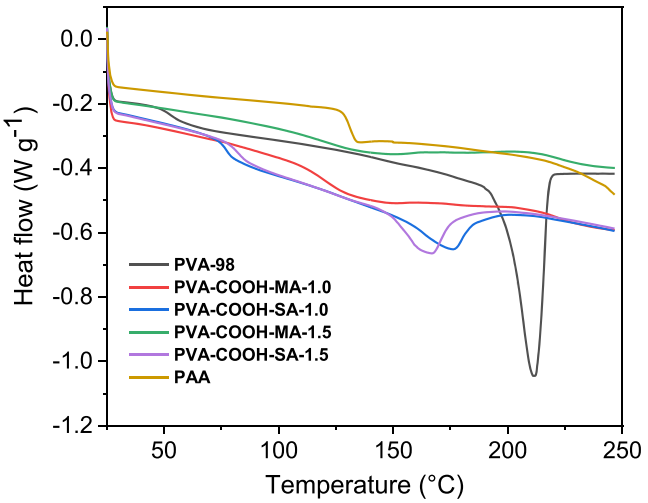

Figure 6. DSC thermograms of PVA, carboxylated PVAs, and PAA (second heating scan).

the pristine PVA-98 shows a large and sharp endothermic peak at 211 °C, which is not seen for the PVA-COOHs. These modified polymers instead show broader melting transitions that are shifted to lower temperatures, indicating smaller crystallites in these materials. In contrast to the semicrystalline PVAs, PAA does not exhibit any other endothermic peak in this temperature range, instead only displaying the glass transition at 131 °C.

From the latent heat of melting (ΔH_m), the degree of crystallinity of the PVA binders was determined by considering a value of ΔH_m = 138.6 J g^{-1} for 100% crystalline PVA,[43] with the results shown in Table 2. The chemical modification of PVA-98 by acid anhydrides obviously leads to a significant decrease in the crystallite size and crystallinity in the modified PVAs. We note that this decrease in crystallinity corresponds well with the reduction in capacity retention seen during cycling (Figure 4). In fact, as seen in Table 2, there is a minimal difference in the melting point and crystallinity among

Table 2. Melting Temperature, Heat of Fusion, and Degree of Crystallinity (X_c) of PVA and Carboxylated PVAs (from the Second Heating Scan)

sample	T_m (°C)	ΔH_m (J g^{-1})	X_c (%)
PVA-98	211	64	46
PVA-COOH-MA-0.5	146	44	32
PVA-COOH-MA-1.0	138	26	19
PVA-COOH-SA-1.0	176	34	25
PVA-COOH-MA-1.5	141	20	14
PVA-COOH-SA-1.5	166	36	26
PVA-COOH-MA-2.0	n/d	n/d	n/d[a]

[a]n/d = not detected.

the different degrees of modification with MA or SA, respectively; this similarity between the materials is directly reflected also in the cycling performance in Figure 4. It thus appears that the degree of crystallinity is a decisive factor for the cycling performance when these PVAs are applied as binders in Si anodes. While the FTIR spectrum (Figure 3) displays a beneficial interaction between the Si nanoparticles and the carboxyl groups of the modified PVAs, this does not seem sufficient to compensate for the loss in crystallinity caused by the structural irregularity upon chemical modification of PVA.

The crystallinity of PVA, being a vinyl polymer, is somewhat of an anomaly since the stereochemical arrangement of the side groups is inherently atactic and the chains lack the stereoregularity normally required for crystallization. Instead, it is the strong intermolecular interactions between the hydrogen-bonding hydroxyl groups that facilitates semicrystallinity in PVA. The semicrystallinity of PVA means that its morphology is a combination of crystalline and amorphous phases. The relative amounts of these phases is a key determinant of the macroscopic properties of the polymer; e.g., when the degree of crystallinity in PVA increases, the stiffness increases, the solubility decreases, and the liquid and gas permeability decreases. These are also properties that may have an influence on the function of the polymer as an electrode binder. Relevant examples from the literature include an increase in the amorphous phase when introducing PAA in a PVA/PAA composite membrane, resulting in a lower mechanical strength for the composite.[44]

From these results, it appears as if any modifications made to the PVA side groups to reduce the hydrogen-bonding abilities of the polymer chains, regardless of the introduced functionality and how minor the modifications are, result in a decrease in crystallinity and a concomitant reduction in cycling performance. To test this hypothesis, PVAs with different degrees of hydrolysis were used as models for investigating the effects of crystallinity separated from any effect of −COOH functionalization. The synthetic origin of commercial PVA means that the material is essentially an acetate-functionalized polymer with different degrees of functionalization. The effects of this functionalization on the cycling performance of the Si anodes were tested using PVAs with three different degrees of hydrolysis (98%, 87−89%, and 80%, referred to as PVA-98, PVA-87, and PVA-80, respectively). On decreasing the degree of hydrolysis, the number of −OH groups in PVA decreases, resulting in a decrease in the hydrogen bonding and disruption of the crystallinity.

As can be seen in the DSC data in Figure S5 and Table 3, the melting point and degree of crystallinity closely follow the degree of hydrolysis for the three PVA samples. A rather dramatic decrease in ΔH_m at lower T_m is observed when the degree of hydrolysis decreases from 98% to 80%. This mimics

Table 3. Melting Temperature, Heat of Fusion, and Degree of Crystallinity (X_c) of Pristine PVAs (from the Second Heating Scan)

sample	T_m (°C)	ΔH_m (J g^{-1})	X_c (%)
PVA-98	211	64	46
PVA-87	178	31	22
PVA-80	164	24	17

https://doi.org/10.1021/acsaem.0c02051
ACS Appl. Energy Mater. 2021, 4, 3008−3016

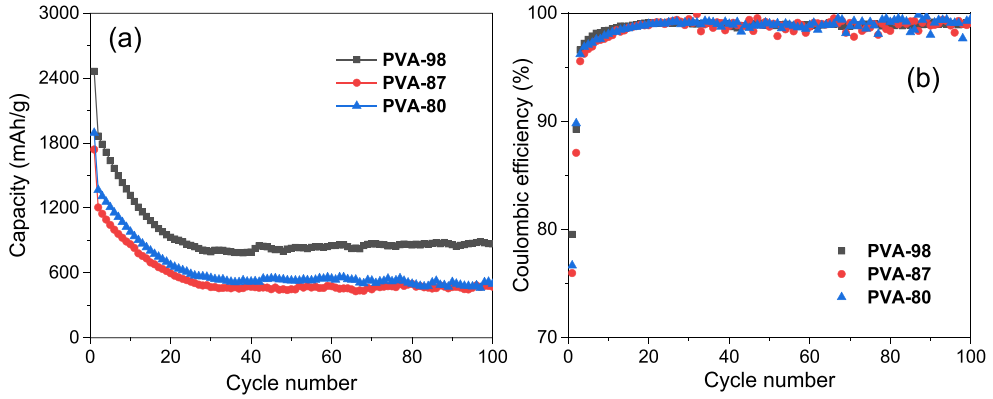

Figure 7. (a) Specific capacity (average of three cells) as a function of cycle number for the Si anode comprising 5 wt % PVA binders at C/20 (1st cycle) and at C/5 (subsequent cycles) and (b) coulombic efficiency plotted as a function of the cycle number.

the effects of the carboxyl functionalization of the MA- and SA-modified PVAs (Figure 4 and Table 2). The materials thus serve well as models with varying degrees of crystallinity as an effect of the functionalization with functional groups that do not specifically interact with the Si active material.

To investigate the effects of the degree of hydrolysis on cycling performance, the PVA-98, -87, and -80 binders were applied in the Si anodes. To emphasize the viability of the binder systems, the cycling tests were carried out using a lower, more commercially relevant binder content (5 wt %) in the Si electrodes and at a C-rate of C/5. The results from these tests are summarized in Figure 7. Individual plots of the average charge capacities of the three cells with standard deviation are shown in Figure S6, and the corresponding capacity values can be found in Table S2. Once again, it can be observed that the PVA-98 electrode exhibits superior cycling performance compared to the other pristine PVAs. The sample shows a stable capacity of 869 mAh g^{-1} after 100 cycles at C/5, compared to 472 and 498 mAh g^{-1} for PVA-87 and PVA-80, respectively. This confirms both PVA-98 as a high-performance binder and the effects of crystallinity on the cycling performance, as we see a similar reduction in the capacity retention for the PVAs with a low degree of hydrolysis as for the modified PVAs.

To highlight that the key performance indicator is indeed the crystallinity, the viscosity of the electrode slurries containing the different binders was determined and is presented in Figures S7 and S8. The binder content corresponds to that used for the electrodes cycled in Figure 4 and Figure 7, respectively. While the slurries with the modified PVAs in Figure S7 show much higher viscosities than the slurries with the unmodified PVAs, there is very little difference between the slurries containing PVAs with different degrees of hydrolysis in Figure S8 despite the clear difference in cycling performance showcased in Figure 7. This effectively rules out slurry rheology and its effect on the electrode processing as a main cause of the observed differences in the cycling performance. It is important to keep in mind that correlation of course does not imply causation and, despite the results presented here, the precise mechanism of the performance variations in these binders remains undetermined. Future studies to investigate the effects of the different binders on the formation of electrochemical degradation layers may possibly shed more light on this.

CONCLUSION

This study has shown the superior performance of using PVA with a high degree of hydrolysis as a binder system for Si-based electrodes, displaying high and stable capacities for extended cycling also for modest binder contents (5 wt %) and moderate currents (C/5). By systematically modifying the type of functionality and degree of functionalization on PVA, it is seen that the surface interactions of the binder with Si do not play a major role for the overall battery performance but that its crystallinity is strongly correlated to the cycling stability, obtained capacity, and coulombic efficiency. This is seen from microscopy analysis, where highly crystalline binders display a better retention of the mechanical integrity during cycling and a limited volume expansion of the Si particles. While chemical modifications of the PVA binder might improve the surface interactions with Si, as seen from FTIR data, they also contribute to a lower degree of crystallinity which in turn worsens the electrode performance.

ASSOCIATED CONTENT

Supporting Information

The Supporting Information is available free of charge at https://pubs.acs.org/doi/10.1021/acsaem.0c02051.

FTIR, TGA, DSC, and average cycling plots and tables for different PVA-based samples (PDF)

AUTHOR INFORMATION

Corresponding Author

Jonas Mindemark − *Department of Chemistry − Ångström Laboratory, Uppsala University, 751 21 Uppsala, Sweden;* orcid.org/0000-0002-9862-7375;
Email: jonas.mindemark@kemi.uu.se

Authors

Prithwiraj Mandal − *Department of Chemistry − Ångström Laboratory, Uppsala University, 751 21 Uppsala, Sweden*

Killian Stokes − *Department of Chemistry − Ångström Laboratory, Uppsala University, 751 21 Uppsala, Sweden*

Guiomar Hernández − *Department of Chemistry − Ångström Laboratory, Uppsala University, 751 21 Uppsala, Sweden;* orcid.org/0000-0002-2004-5869

Daniel Brandell − *Department of Chemistry − Ångström Laboratory, Uppsala University, 751 21 Uppsala, Sweden;* orcid.org/0000-0002-8019-2801

Complete contact information is available at:

https://pubs.acs.org/10.1021/acsaem.0c02051

Notes

The authors declare no competing financial interest.

■ ACKNOWLEDGMENTS

Financial support from the Swedish Energy Agency project "SiLiCOAT" (Grant Number 40466-1) and STandUP for Energy is gratefully acknowledged. Rassmus Andersson is acknowledged for the preparation of Si electrodes.

■ REFERENCES

(1) Nitta, N.; Wu, F.; Lee, J. T.; Yushin, G. Li-ion battery materials: present and future. *Mater. Today* **2015**, *18* (5), 252−264.
(2) Tarascon, J. M.; Armand, M. Issues and challenges facing rechargeable lithium batteries. *Nature* **2001**, *414* (6861), 359−367.
(3) Antolini, E. LiCoO2: formation, structure, lithium and oxygen nonstoichiometry, electrochemical behaviour and transport properties. *Solid State Ionics* **2004**, *170* (3), 159−171.
(4) Kim, J.-H.; Kim, J.-S.; Lim, Y.-G.; Lee, J.-G.; Kim, Y.-J. Effect of carbon types on the electrochemical properties of negative electrodes for Li-ion capacitors. *J. Power Sources* **2011**, *196* (23), 10490−10495.
(5) Zhang, W.-J. A review of the electrochemical performance of alloy anodes for lithium-ion batteries. *J. Power Sources* **2011**, *196* (1), 13−24.
(6) Ashuri, M.; He, Q.; Shaw, L. L. Silicon as a potential anode material for Li-ion batteries: where size, geometry and structure matter. *Nanoscale* **2016**, *8* (1), 74−103.
(7) Franco Gonzalez, A.; Yang, N.-H.; Liu, R.-S. Silicon Anode Design for Lithium-Ion Batteries: Progress and Perspectives. *J. Phys. Chem. C* **2017**, *121* (50), 27775−27787.
(8) Li, J.-Y.; Xu, Q.; Li, G.; Yin, Y.-X.; Wan, L.-J.; Guo, Y.-G. Research progress regarding Si-based anode materials towards practical application in high energy density Li-ion batteries. *Mater. Chem. Front.* **2017**, *1* (9), 1691−1708.
(9) Chan, C. K.; Peng, H.; Liu, G.; McIlwrath, K.; Zhang, X. F.; Huggins, R. A.; Cui, Y. High-performance lithium battery anodes using silicon nanowires. *Nat. Nanotechnol.* **2008**, *3* (1), 31−35.
(10) Zamfir, M. R.; Nguyen, H. T.; Moyen, E.; Lee, Y. H.; Pribat, D. Silicon nanowires for Li-based battery anodes: a review. *J. Mater. Chem. A* **2013**, *1* (34), 9566−9586.
(11) Park, M.-H.; Kim, M. G.; Joo, J.; Kim, K.; Kim, J.; Ahn, S.; Cui, Y.; Cho, J. Silicon Nanotube Battery Anodes. *Nano Lett.* **2009**, *9* (11), 3844−3847.
(12) Cui, L.-F.; Ruffo, R.; Chan, C. K.; Peng, H.; Cui, Y. Crystalline-Amorphous Core-Shell Silicon Nanowires for High Capacity and High Current Battery Electrodes. *Nano Lett.* **2009**, *9* (1), 491−495.
(13) Chen, Y.; Hu, Y.; Shen, Z.; Chen, R.; He, X.; Zhang, X.; Li, Y.; Wu, K. Hollow core−shell structured silicon@carbon nanoparticles embed in carbon nanofibers as binder-free anodes for lithium-ion batteries. *J. Power Sources* **2017**, *342*, 467−475.
(14) Jia, H.; Zheng, J.; Song, J.; Luo, L.; Yi, R.; Estevez, L.; Zhao, W.; Patel, R.; Li, X.; Zhang, J.-G. A novel approach to synthesize micrometer-sized porous silicon as a high performance anode for lithium-ion batteries. *Nano Energy* **2018**, *50*, 589−597.
(15) Sakabe, J.; Ohta, N.; Ohnishi, T.; Mitsuishi, K.; Takada, K. Porous amorphous silicon film anodes for high-capacity and stable all-solid-state lithium batteries. *Commun. Chem.* **2018**, *1* (1), 24.
(16) Sohn, M.; Lee, D. G.; Park, H.-I.; Park, C.; Choi, J.-H.; Kim, H. Microstructure Controlled Porous Silicon Particles as a High Capacity Lithium Storage Material via Dual Step Pore Engineering. *Adv. Funct. Mater.* **2018**, *28* (23), 1800855.
(17) Komaba, S.; Shimomura, K.; Yabuuchi, N.; Ozeki, T.; Yui, H.; Konno, K. Study on Polymer Binders for High-Capacity SiO Negative Electrode of Li-Ion Batteries. *J. Phys. Chem. C* **2011**, *115* (27), 13487−13495.
(18) Erk, C.; Brezesinski, T.; Sommer, H.; Schneider, R.; Janek, J. Toward Silicon Anodes for Next-Generation Lithium Ion Batteries: A Comparative Performance Study of Various Polymer Binders and Silicon Nanopowders. *ACS Appl. Mater. Interfaces* **2013**, *5* (15), 7299−7307.
(19) Wang, C.; Wu, H.; Chen, Z.; McDowell, M. T.; Cui, Y.; Bao, Z. Self-healing chemistry enables the stable operation of silicon microparticle anodes for high-energy lithium-ion batteries. *Nat. Chem.* **2013**, *5* (12), 1042−1048.
(20) Mazouzi, D.; Karkar, Z.; Reale Hernandez, C.; Jimenez Manero, P.; Guyomard, D.; Roué, L.; Lestriez, B. Critical roles of binders and formulation at multiscales of silicon-based composite electrodes. *J. Power Sources* **2015**, *280*, 533−549.
(21) Jeschull, F.; Lacey, M. J.; Brandell, D. Functional binders as graphite exfoliation suppressants in aggressive electrolytes for lithium-ion batteries. *Electrochim. Acta* **2015**, *175*, 141−150.
(22) Jeschull, F.; Lindgren, F.; Lacey, M. J.; Björefors, F.; Edström, K.; Brandell, D. Influence of inactive electrode components on degradation phenomena in nano-Si electrodes for Li-ion batteries. *J. Power Sources* **2016**, *325*, 513−524.
(23) Karkar, Z.; Guyomard, D.; Roué, L.; Lestriez, B. A comparative study of polyacrylic acid (PAA) and carboxymethyl cellulose (CMC) binders for Si-based electrodes. *Electrochim. Acta* **2017**, *258*, 453−466.
(24) Chartrel, T.; Ndour, M.; Bonnet, V.; Cavalaglio, S.; Aymard, L.; Dolhem, F.; Monconduit, L.; Bonnet, J.-P. Revisiting and improving the preparation of silicon-based electrodes for lithium-ion batteries: ball milling impact on poly(acrylic acid) polymer binders. *Mater. Chem. Front.* **2019**, *3* (5), 881−891.
(25) Bresser, D.; Buchholz, D.; Moretti, A.; Varzi, A.; Passerini, S. Alternative binders for sustainable electrochemical energy storage − the transition to aqueous electrode processing and bio-derived polymers. *Energy Environ. Sci.* **2018**, *11* (11), 3096−3127.
(26) Li, J.-T.; Wu, Z.-Y.; Lu, Y.-Q.; Zhou, Y.; Huang, Q.-S.; Huang, L.; Sun, S.-G. Water Soluble Binder, an Electrochemical Performance Booster for Electrode Materials with High Energy Density. *Adv. Energy Mater.* **2017**, *7* (24), 1701185.
(27) Magasinski, A.; Zdyrko, B.; Kovalenko, I.; Hertzberg, B.; Burtovyy, R.; Huebner, C. F.; Fuller, T. F.; Luzinov, I.; Yushin, G. Toward Efficient Binders for Li-Ion Battery Si-Based Anodes: Polyacrylic Acid. *ACS Appl. Mater. Interfaces* **2010**, *2* (11), 3004−3010.
(28) Parikh, P.; Sina, M.; Banerjee, A.; Wang, X.; D'Souza, M. S.; Doux, J.-M.; Wu, E. A.; Trieu, O. Y.; Gong, Y.; Zhou, Q.; Snyder, K.; Meng, Y. S. Role of Polyacrylic Acid (PAA) Binder on the Solid Electrolyte Interphase in Silicon Anodes. *Chem. Mater.* **2019**, *31* (7), 2535−2544.
(29) Lestriez, B.; Bahri, S.; Sandu, I.; Roué, L.; Guyomard, D. On the binding mechanism of CMC in Si negative electrodes for Li-ion batteries. *Electrochem. Commun.* **2007**, *9* (12), 2801−2806.
(30) Li, J.; Lewis, R. B.; Dahn, J. R. Sodium Carboxymethyl Cellulose. *Electrochem. Solid-State Lett.* **2007**, *10* (2), A17.
(31) Park, H.-K.; Kong, B.-S.; Oh, E.-S. Effect of high adhesive polyvinyl alcohol binder on the anodes of lithium ion batteries. *Electrochem. Commun.* **2011**, *13* (10), 1051−1053.
(32) Nguyen, C. C.; Yoon, T.; Seo, D. M.; Guduru, P.; Lucht, B. L. Systematic Investigation of Binders for Silicon Anodes: Interactions of Binder with Silicon Particles and Electrolytes and Effects of Binders on Solid Electrolyte Interphase Formation. *ACS Appl. Mater. Interfaces* **2016**, *8* (19), 12211−12220.
(33) Jeena, M. T.; Lee, J.-I.; Kim, S. H.; Kim, C.; Kim, J.-Y.; Park, S.; Ryu, J.-H. Multifunctional Molecular Design as an Efficient Polymeric Binder for Silicon Anodes in Lithium-Ion Batteries. *ACS Appl. Mater. Interfaces* **2014**, *6* (20), 18001−18007.
(34) He, J.; Zhang, L. Polyvinyl alcohol grafted poly (acrylic acid) as water-soluble binder with enhanced adhesion capability and electrochemical performances for Si anode. *J. Alloys Compd.* **2018**, *763*, 228−240.
(35) Kovalenko, I.; Zdyrko, B.; Magasinski, A.; Hertzberg, B.; Milicev, Z.; Burtovyy, R.; Luzinov, I.; Yushin, G. A Major Constituent of Brown Algae for Use in High-Capacity Li-Ion Batteries. *Science* **2011**, *334* (6052), 75.

(36) Ryou, M.-H.; Kim, J.; Lee, I.; Kim, S.; Jeong, Y. K.; Hong, S.; Ryu, J. H.; Kim, T.-S.; Park, J.-K.; Lee, H.; Choi, J. W. Mussel-Inspired Adhesive Binders for High-Performance Silicon Nanoparticle Anodes in Lithium-Ion Batteries. *Adv. Mater.* **2013**, *25* (11), 1571−1576.
(37) Song, J.; Zhou, M.; Yi, R.; Xu, T.; Gordin, M. L.; Tang, D.; Yu, Z.; Regula, M.; Wang, D. Interpenetrated Gel Polymer Binder for High-Performance Silicon Anodes in Lithium-ion Batteries. *Adv. Funct. Mater.* **2014**, *24* (37), 5904−5910.
(38) Wang, L.; Gao, B.; Peng, C.; Peng, X.; Fu, J.; Chu, P. K.; Huo, K. Bamboo leaf derived ultrafine Si nanoparticles and Si/C nanocomposites for high-performance Li-ion battery anodes. *Nanoscale* **2015**, *7* (33), 13840−13847.
(39) Wang, L.; Liu, T.; Peng, X.; Zeng, W.; Jin, Z.; Tian, W.; Gao, B.; Zhou, Y.; Chu, P. K.; Huo, K. Highly Stretchable Conductive Glue for High-Performance Silicon Anodes in Advanced Lithium-Ion Batteries. *Adv. Funct. Mater.* **2018**, *28* (3), 1704858.
(40) Bunn, C. W. Crystal Structure of Polyvinyl Alcohol. *Nature* **1948**, *161* (4102), 929−930.
(41) Holland, B. J.; Hay, J. N. The thermal degradation of poly(vinyl alcohol). *Polymer* **2001**, *42* (16), 6775−6783.
(42) Thomas, D.; Cebe, P. Self-nucleation and crystallization of polyvinyl alcohol. *J. Therm. Anal. Calorim.* **2017**, *127* (1), 885−894.
(43) Rahman Khan, M. M.; Pal, S.; Hoque, M. M.; Alam, M. R.; Younus, M.; Kobayashi, H. Simple Fabrication of PVA−ZnS Composite Films with Superior Photocatalytic Performance: Enhanced Luminescence Property, Morphology, and Thermal Stability. *ACS Omega* **2019**, *4* (4), 6144−6153.
(44) Wu, G. M.; Lin, S. J.; Yang, C. C. Preparation and characterization of PVA/PAA membranes for solid polymer electrolytes. *J. Membr. Sci.* **2006**, *275* (1), 127−133.

https://doi.org/10.1021/acsaem.0c02051
ACS Appl. Energy Mater. 2021, 4, 3008−3016